JOURNAL OF COMPUTATIONAL PHYSICS **130,** 256–265 (1997)
ARTICLE NO. CP965585

The Phase-Field Method in the Sharp-Interface Limit: A Comparison between Model Potentials

M. Fabbri*,[1] and V. R. Voller†

*Núcleo de Desenvolvimento Tecnológico, Universidade São Francisco, Itatiba, SP 13.251-900, Brazil; †Department of Civil and Mineral Engineering, University of Minnesota, Minneapolis, Minnesota 55455

Received April 11, 1996; revised September 10, 1996

The phase-field (PF) method for solidification phenomena is an open formulation based on a free-energy functional. Two common choices for the PF potential, here referred to briefly as the Caginalp and Kobayashi models, are compared with respect to their numeric results within the classical sharp-interface limit. Both qualitative and quantitative behavior are addressed, and an assessment of the computational effort required to approximate a sharp-interface problem is made. It is shown that the specific form of the free-energy potential does have a strong influence on the convergence of the PF results to their sharp-interface limit. Compliance of the PF solutions with the linear kinetic model for the interface temperature is also investigated. A simple one-dimensional solidification problem in the presence of kinetic undercooling is solved by the PF model and also by a deforming grid method. Our results support the view that, if care is exercised in formulating the phase–temperature coupling, there is a high degree of confidence in using the PF method for the numerical modeling of general solidification phenomena.

1. INTRODUCTION

Recently, phase field (PF) methods have become increasingly attractive for the numerical simulation of solidification phenomena. By establishing the convergence properties of the PF equations as related to their sharp-interface model counterparts, the analysis and numerical studies of Caginalp and coworkers [1–3] have provided the free-energy formulation, best known in the physics community through the papers of Langer [4] and Collins and Levine [5], with a solid mathematical basis. Computer simulations by Kobayashi [6] on anisotropic dendritic growth in a pure undercooled melt reveals (with a fairly moderate computational effort) a richness of details, at the ''microscopic'' scale, in which the roles played by surface tension and kinetic effects are fully taken into account. In a recent series of papers, Wheeler, Boettinger, and McFadden [7, 8] have applied the standard PF method to binary mixtures, and more recently, Caginalp and coworkers [9, 10] have obtained and analyzed a PF formulation suitable for dilute thermal alloys. Finally, with the ongoing efforts to arrive at a rigorous thermodynamic formulation for nonisothermal systems [11] and to encompass fluid-flow phenomena [12], the PF technique is likely to offer a practical alternative to the more traditional (and cumbersome) interface-tracking methods.

The basic PF equation arises from the classical Landau theories of phase transitions by considering a first-order expansion of the free energy density in the ''order parameter'' p:

$$\mathscr{F} = \int \left\{ \frac{1}{2}\xi^2 |\nabla p|^2 + F(p,u) \right\} d^3r. \tag{1.1}$$

$F(p, u)$ is a double-well potential having local minima at the p-values corresponding to the two possible choices of the phase state at the bulk (solid or liquid), while ξ is a gradient-energy coefficient which is proportional to the interface length scale. In a general model, u can be any relevant intensive property; in the present context, u will denote temperature. The time evolution of p is assumed to obey a simple linear kinetic relationship

$$\tau \frac{\partial p}{\partial t} = -\frac{\delta \mathscr{F}}{\delta p} \tag{1.2}$$

which is the common procedure employed in mean field theories of critical phenomena [13] (there is no special concern here about ''critical points,'' since the solid and liquid phases are always assumed to be distinct).

As for the evolution of temperature, we adopt the common procedure for treating energy conservation, which leads to the usual time-dependent heat equation plus a source term (representing the latent-heat release at the interface); this is an ''ad-hoc'' assumption about the phase-temperature coupling, which nevertheless has been shown to yield the correct qualitative behavior of complex phase-front patterns during dendritic solidification [6, 14].

[1] Permanent Address: Instituto Nacional de Pesquisas Espaciais, Laboratorio de Materiais e Sensores, C.P.515, 12225-970 São José dos Campos, SP, Brasil.

0021-9991/97 $25.00

It should be mentioned that Penrose and Fife [11] have proposed a thermodynamically consistent PF formulation based on the entropy functional and called attention to the fact that the free energy does not need to decrease along the solution paths in the case of nonisothermal systems. In fact, though the PF equations are a direct consequence of a few well-established statistical mechanics principles, their specific "thermodynamically consistent" realizations are still open to research. The interested reader is urged to follow the discussions initiated in Ref. [11].

The PF equations embody a physically realistic model for solidification, which is lacking in the mathematical sharp-interface (Stefan) formulation. Nevertheless, due to the intrinsic complicated nature of the microscopic solidification phenomena, it is difficult to access the correctness of PF numerical results quantitatively. Lowen, Bechhoefer, and Tuckerman [15] have addressed the transition from diffusive to kinetic-dominated regimes, through a series of PF numerical simulations, but a quantitative comparison of their results with carefully devised experiments on plane-front solidification of alloys is lacking. Caginalp and Sokolovsky [3] have compared the results of their PF model against the classical sharp-interface limit, where analytic results are available in the absence of kinetic or surface tension effects. The state of affairs is complicated when one realizes that the PF equations are not unique, in the sense that one is free to choose the actual form of the potential, as long as it preserves the basic properties which gives rise to the phase transition; hence it might be possible to generate different numeric results by choosing alternative forms for $F(p, u)$.

In the present work, we take a close look at some numerical results obtained with the PF approach, aiming at a quantitative comparison between two common choices for the coupling potential $F(p, u)$, viz. the Caginalp [1] and the Kobayashi [6] forms, hereafter referred as the CP and KP models, respectively. As a "bench mark," we also relate the numerical results with their expected classical sharp-interface solutions. The classical solution will include the limiting analytical solution for the Stefan problem, and a numerical solution based on a deforming grid for plane-front kinetic undercooling. The objective of using the benchmark solution is to provide a crude, but useful, criteria as to how much computational effort is required to describe quantitatively a sharp-interface solidification problem with the PF equations. In this comparison both the convergence properties, and the numerical error expected by employing a finite-thickness interface in the PF equations will be investigated. For the same computational effort, and for practical values of the kinetic coefficient, we shall see that KP compares more favorably with the sharp interface results, although both KP and CP yield the same qualitative behavior. Furthermore, for large values of the kinetic coefficient, the results of the PF equations seem to have a strong dependence on the actual form employed for the potential $F(p, u)$.

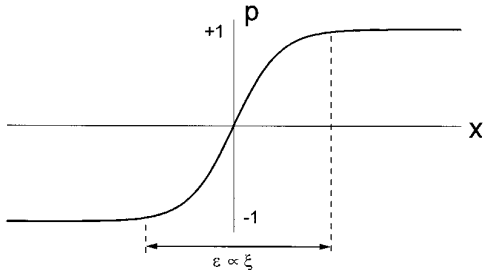

FIG. 1. Expected spatial profile of the phase-field through a solid–liquid interface.

2. BASIC MODELS

2.1. The Sharp Interface Model Problem

On the microscopic scale, the classical solidification problem is described as a moving-boundary problem in heat transport; the conditions at the interface $\Gamma(t)$ are the Stefan (latent heat release) and the extended Gibbs–Thomson relations (we hereafter assume a unit, constant, volumetric specific heat, $\rho C = 1$):

$$\frac{\partial u}{\partial t} = K\nabla^2 u \qquad \text{in } \Omega/\Gamma(t) \tag{2.1a}$$

$$Lv = -K[\nabla u]^{+}_{-} \qquad \text{in } \Gamma(t) \tag{2.1b}$$

$$u = -\frac{\sigma}{\Delta s}(k + \alpha v) \quad \text{in } \Gamma(t). \tag{2.1c}$$

Δs is the entropy scale, which is defined as the difference between the entropies of the liquid and solid at the melting temperature ($\Delta s = L/T_m$). The kinetic parameter is $(\alpha\sigma/\Delta s)$, and k is the local interface curvature.

By allowing $\sigma \to 0$, we obtain the classical Stefan problem. The case $\sigma \neq 0$, $\alpha \neq 0$, and $k = 0$ is referred as the modified Stefan problem; the condition $k = 0$ describes plane-front solidification.

2.2 The Phase-Field (PF) Equations

The PF approach avoids the explicit treatment of the interface conditions (2.1b) and (2.1c). One solves instead a coupled nonlinear system of evolution equations for the phase p and temperature u fields:

$$\alpha\xi^2 \frac{\partial p}{\partial t} = \xi^2 \nabla^2 p - \frac{\partial F}{\partial p} \tag{2.2a}$$

$$\frac{\partial u}{\partial t} + \frac{1}{2} L \frac{\partial p}{\partial t} = K\nabla^2 u. \tag{2.2b}$$

We adopt the convention that $p = +1$ refers to liquid and $p = -1$ to the solid phase. The interface region, of length $\sim\xi$, corresponds to intermediate values of p (Fig. 1).

The above set of equations has a simple dynamic interpretation. The phase equation (2.2a) is just a linear time evolution governed by the imbalance between the excess interface free-energy and the restoring potential $F(p, u)$. The Fourier heat conduction equation (2.2b) has a source term to account for the latent heat release at the moving interface.

If the PF equations are to be employed to simulate real solidification problems, one should expect that the interface conditions (2.1b), (2.1c) must be satisfied by the solutions of (2.2a), (2.2b), as the interface thickness $\xi \to 0$. Unfortunately, general results, based only on the thermodynamic consistency of $F(p, u)$, are lacking. The work of Caginalp [1], however, provides a strong indication that the usual sharp-interface limit is attained for all forms of the free-energy potential $F(p, u)$ in which the p–u coupling is linear (i.e., $\partial^2 F/\partial p\,\partial u = 0$).

Given a specific form of $F(p, u)$, the entropy/energy/temperature scales must obey the relationships:

$$\Delta s = (S_{\text{liquid}} - S_{\text{solid}}) = \frac{\partial F}{\partial u}\bigg|_{\text{sol}}^{\text{liq}} \tag{2.3a}$$

$$\Delta s|_{u=0} = \frac{L}{T_m}. \tag{2.3b}$$

Note that the above relations can be used to define a convenient entropy scale Δs, such that the actual (non-scaled) values of temperature and latent heat are employed in Eqs. (2.2a), (2.2b).

The (temperature-dependent) surface tension σ, which is obtained from the excess free energy at the interface region, can be expressed solely in terms of the potential $F(p, u)$ (see, e.g., [16]), yielding

$$\sigma = \xi 2^{1/2} \int_{-1}^{+1} F(p, u)^{1/2}\, dp. \tag{2.4}$$

Allen and Cahn [16] have shown that the above relation remains valid if one neglects the curvature influence on the phase field profile at the interface region.

The practical usefulness of the PF equations relies on the assumption that numerical solutions, obtained from (2.2a), (2.2b) for a finite value of the interfacial thickness ξ, are good approximations for the sharp-interface solutions of (2.1a)–(2.1c). As for the potential $F(p, u)$, we consider here two possible simple choices, best known in the literature through the works of Caginalp and Kobayashi.

2.2.1. *The Caginalp Potential* (*CP*)

In the CP model, the dependence of F on u is taken into account through a simple linear term added to the double-well potential:

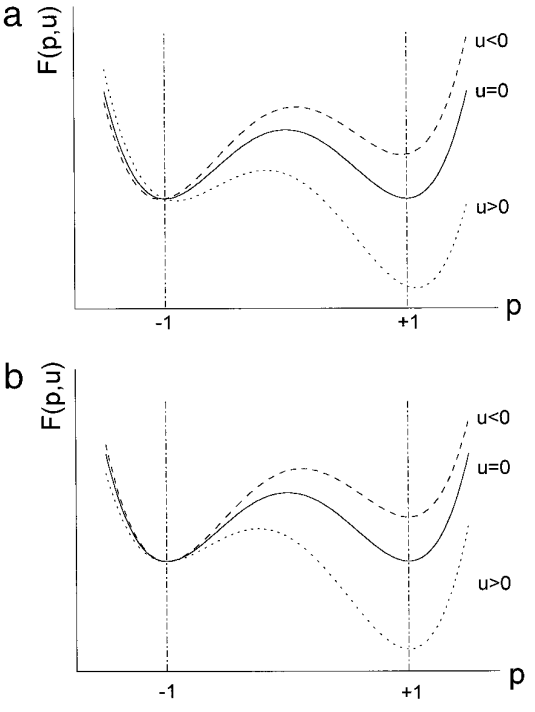

FIG. 2. Double-well-potentials as prescribed by the CP (a, Caginalp) and the KP (b, Kobayashi) models.

$$F(p, u) = \frac{1}{8a}(p^2 - 1)^2 - \frac{\Delta s}{2} pu. \tag{2.5}$$

The parameter a must be chosen such that $\partial F/\partial p$ exhibits three distinct roots, near 0 and ± 1. Application of formula (2.4) leads to the value of σ at $u = 0$:

$$\sigma = \frac{2}{3}\frac{\xi}{\sqrt{a}}. \tag{2.6}$$

The prescription (2.5) implies that the minima of $F(p, u)$ shifts from ± 1 continuously as u departs from 0 (Fig. 2a). For a finite value of a, this implies that a small amount of latent heat is released at positions away from the interface (see Eq. (2.2b)). This undesirable effect clearly fades out as $a \to 0$. Indeed, Caginalp and coworkers [1–3, 17] have established the convergence of the PF/CP equations to the correct sharp-interface limit as both $\xi \to 0$ and $a \to 0$.

2.2.2. *The Kobayashi Potential* (*KP*)

The KP model (Fig. 2b) employs a fourth-degree polynomial for F, with fixed minima at ± 1:

$$F(p, u) = \frac{W}{16} \int_0^p (1 - \Phi^2)[\Phi + 2b(u)]\, d\Phi. \tag{2.7}$$

$b(u)$ is a monotonic increasing function of temperature satisfying $|b(u)| < \frac{1}{2}$; it is also desirable to have $b(u)$ of order u for $u \sim 0$, since that makes the entropy difference between solid and liquid a linear function of u, around the melting temperature. Following Wheeler *et al.* [7], we employ a simple linear form for $b(u)$, which proved adequate during applications of the PF model to binary alloys:

$$b(u) = \frac{6\Delta s}{W} u. \tag{2.8}$$

The value of σ at $u = 0$ is then given by

$$\sigma = \frac{\xi}{3}\left(\frac{W}{2}\right)^{1/2}. \tag{2.9}$$

Since the p–u coupling prescribed by (2.7) is nonlinear, no rigorous properties are known for the KP model, concerning its limit as $\xi \to 0$; however, a reasonable physical argument provided by Kobayashi [6, 18] asserts its convergence to the expected classical sharp-interface results. Furthermore, the numerical results we are about to present suggest that the KP model approaches faster than CP's the classical sharp-interface limit. Wheeler *et al.* [19] have also checked the numerical behavior of the KP model in one- and two-dimensional space.

2.2.3. *Other Choices and Improvements*

The CP model equation (2.5) and KP's, Eq. (2.7), were considered here due to their relative simplicity, which make them natural choices for a first PF implementation. It should be stressed, though, that other forms of the PF potential, as well as improved forms of the PF equations, have been proposed and investigated by Wang *et al.* [20] and Caginalp and Chen [21], among others. These alternative choices seek thermodynamic consistency (e.g., the use of a proper entropy functional), allied to better numerical and convergence properties. We recommend Ref. [20] for a clear overview and discussion.

3. NUMERIC SIMULATIONS

3.1. The Prototype Problem

Following Caginalp and Socolovsky [3], we consider the simple one-dimensional solidification of a pure substance, with $K = L = 1$, over a semi-infinite domain. The corresponding classical Stefan problem is given by Eqs. (2.1) with $\Omega = [0, \infty)$, and $\sigma = 0$. Initially, the whole domain is at $u = T_{\text{hot}} = 0.015$, except at $x = 0$, where it is held fixed at $u = T_{\text{cold}} = -0.085$. The analytic solution to that problem is well known [22]; in particular, the interface position will advance according to

$$\Gamma(t) = 0.396618 t^{1/2}. \tag{3.1}$$

The temperature field and the temperature history at any time or position can also be obtained from the Neuman analytic solution [22].

3.2. Kinetic Undercooling Effects

In order to avoid velocity discontinuities at the interface, the effect of a nonzero kinetic coefficient ($\sigma \neq 0$ and $\alpha \neq 0$ in Eqs. (2.1)) is numerically investigated as follows. From $t = 0$ to $t = t_0$, a simple Stefan solidification with $\alpha \approx 0$ is assumed; at $t_0 = 0.1846$, the interface $\Gamma(t)$, as prescribed by (3.1), has reached the position $x_0 = 0.14$, and its velocity is $v_0 = 0.4616$. For $t > t_0$, we look at the progression of the numeric solution for the desired value of $\alpha \neq 0$. According to Eq. (2.1c), the temperature at the interface should be given by

$$-T^0 = -\frac{\alpha\sigma}{\Delta s} v_0. \tag{3.2}$$

Our approach is to solve numerically the PF equations (2.2), with the initial condition for u as prescribed by the analytic Newman solution for the sharp interface problem at $t = t_0$; in this manner, the kinetic undercooling effect is suddenly triggered at $t = t_0$ (which resembles the sudden appearance of facets during the growth of crystal grains). The idea is to investigate numerically the validity of the relationship (3.2), which would be an explicit condition imposed at the interface in the classical sharp model formulation, but which is expected to hold for PF solutions only in the limit of zero interface thickness. The interface velocity $d\Gamma/dt$ is obtained from the numerical solution by simple numerical differentiation.

3.3. Domain of Integration, Initial, and Boundary Conditions

We consider the numerical solution of Eqs. (2.2) in the domain $x_0 < x < 1.0$, $t_0 < t < 2.0$. Let $u_s(x, t)$ be the analytic solution of the prototype sharp-interface classical Stefan problem, as described in (3.1) above. Then the boundary and initial conditions for temperature are

$$u(0, t) = T_{\text{cold}}$$
$$u(1, t) = u_s(1, t)$$
$$u(x, t_0) = u_s(x, t_0).$$

The initial and boundary conditions for p must be chosen accordingly to the physical requirements of each model. For the CP model, we have

$p(x, t_0)$ = minimum of $F[p, u_s(x, t_0)]$

$$\text{closest to} \begin{cases} -1, & \text{for } x \le x_0; \\ +1, & \text{for } x > x_0; \end{cases}$$

$p(0, t)$ = minimum of $F[p, T_{\text{cold}}]$ closest to -1;

$p(1, t)$ = minimum of $F[p, u_s(1, t)]$ closest to $+1$.

For the KP model, these conditions reduce to

$$\begin{aligned} p(x, t_0) &= -1, \quad \text{for } x \le x_0; \\ &\quad +1, \quad \text{for } x > x_0; \\ p(0, t) &= -1; \\ p(1, t) &= +1. \end{aligned}$$

We were not particularly careful about the discontinuity in the initial value imposed for the phase field. Our numeric experiments indicate that there is little (if any) improvement if an alternative initial smoothed function is employed for $p(x, t)$.

3.4. Method of Solution

We discretize Eqs. (2.2) by a simple totally implicit, finite difference scheme over a fixed and uniform spatial grid (first-order in time, second-order in space). The nonlinear term in the p equation was treated by the source-linearization method of Patankar [23]; then the coupled system of discretized equations obtained from (2.2a), (2.2b) are solved iteratively. A constant overrelaxation value of 1.7 was enough to attain convergence in all runs. This is perhaps the simplest possible efficient numerical scheme one can devise to solve the PF equations; the even simpler explicit scheme becomes prohibitive at the small spatial mesh sizes required to handle the stiffness of the p equation for small values of ξ. A good improvement would be to consider an adaptive method, which nevertheless would require a carefully designed algorithm to handle multiple connected interfaces at higher dimensions. We shall consider such refinements in a future work. The fixed-uniform grid discretization is also directly amenable to optimization in vector and parallel computers.

Lin [24] has employed a double-fixed-grid method, where an implicit discretization of the temperature equation in a coarse mesh is superimposed to an explicit discretization of the phase equation over a finer grid. We decided that a totally implicit scheme with source linearization is more adequate for our purposes here, since we are looking for a precise value of the temperature at the phase front.

3.5. Other Numerical Settings

Previous experience with numerical solutions of the PF equations [2, 3, 6, 7, 14, 15] have shown that the interface thickness ε (the region of space where p exhibit large gradients) is usually larger than ξ (typical values for the KP model, and for the CP model with $a = 1$ are between ξ and 10ξ). Since the fixed grid method currently employed only makes sense when the mesh space Δx is smaller than ε, we always take $\xi = 1.25\Delta x$:

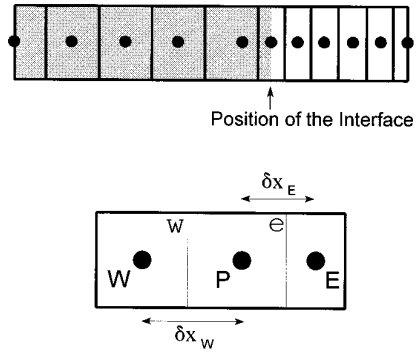

FIG. 3. Detail of the spatial grid employed in the deforming grid method, also showing the notation scheme.

$$\xi = 1.25/N \tag{3.3}$$

where N is the number of spatial intervals in the domain $0.0 < x < 1.0$.

The comparison between the results obtained with both potential models is done with respect to a common scale of units; by choosing $\Delta s = 4.0$, $a = 1.0$ for the CP model, and $W = 8.0$ for the KP model, we ensure that, for the same N, both models are solved for the same value of σ and ξ (see (2.6) and (2.9)).

In what follows, we shall refer to ξ simply as the "interface thickness," meaning that the actual spatial length of the "numerical" interface, ε, is of order ξ for $\xi \to 0$.

3.6. A Deforming-Grid Method

As a bench mark for comparison, a numerical solution to the classical modified Stefan problem is obtained by a front-tracking deforming-grid method. This approach is an extension of the deforming grid method recently reported by Voller and Peng [25]. The computational region, $0 < x < 1$, is covered by a grid of N node points. Initially at time t_0, the grid is constructed so that the solid/liquid interface, at $x = 0.14$, is located on a selected internal node, labeled *nf*. As the problem evolves the grid is continuously deformed so that (i) the interface always remains on node *nf* and (ii) the grid spacing in the solid and liquid regions is uniform. Figure 3 shows a schematic "snap shot" of the grid at a given point of time in the calculation. Note the labeling convention, i.e., upper case letters (W, P, E) refer to the node points and lower case letters (e, w) refer to the locations of the dividing grid lines between node points.

Using a fully implicit finite difference integration in time, the heat balance on the deforming grid in Fig. 3, for the given test problem and thermal data, can be written as

$$\left[\Delta x + \frac{\Delta t}{\delta x_W} + \frac{\Delta t}{\delta x_E} + \Delta t \frac{v_w - v_e}{2}\right] T_P = \Delta x^{\text{old}} T_P^{\text{old}} + \left[\frac{\Delta t}{\delta x_E} + \frac{\Delta t v_e}{2}\right] T_E + \left[\frac{\Delta t}{\delta x_W} - \frac{\Delta t v_w}{2}\right] T_W + S_P, \quad (3.4)$$

where

$$\Delta x = \frac{\delta x_E}{2} + \frac{\delta x_W}{2}, \quad (3.5)$$

v_e and v_w are the velocities of the grid lines, and

$$S_P = \begin{cases} 0, & \text{if } P < nf \\ v_e + \dfrac{\Delta x^{\text{old}}}{2} - \dfrac{\Delta x}{2}, & \text{if } P = nf \\ v_e - v_w + \Delta x^{\text{old}} - \Delta x, & \text{if } P > nf. \end{cases} \quad (3.6)$$

The iterative solution of (3.4) on the deforming grid, in a given time step, is as follows: The iteration is initiated on setting the current grid spacing to the old time step value. After a tridiagonal solution of Eq. (3.4), the grid spacing is updated for the next iteration by interpolating for the undercooled isotherm in the predicted nodal temperature field and relocating the position of the interface node (node nf).

Note that:

1. The undercooled temperature is readily calculated by approximating the velocity of the interface node as

$$v_{\text{interface}} = \frac{x_p - x_p^{\text{old}}}{\Delta t} \quad (3.7)$$

and then employing Eq. (2.1c).

2. The calculation of the interface velocity and the updating of the grid often requires some underrelaxation, particularly when small time steps are employed.

Typical runs with the deforming grid method were made employing an 80-point mesh, with a time step of 0.005; the processor time is about 0.05 s per time step using a PC-AT486/DX2/50MHz computer.

4. RESULTS

We considered four values for the initial undercooling temperature T_0:

- 0.0002: A fairly small value, aiming at reproducing the results of the simple Stefan sharp-interface problem;
- 0.002; 0.02: which correspond to values for the kinetic coefficient encountered during actual solidification experiments;
- 0.08: a high value, to push to the extreme the consequences of the nonlinear p–u coupling in the free-energy model.

The numerical integration was carried out with a number of grid sizes $N = 100$, 250, 500, 1000, and, in some cases, $N = 2000$. Typical processor times are shown in Table I.

4.1. Interface Progression

Figures 4a,b compare the calculated interface position $\Gamma(t)$, for nearly zero initial undercooling ($T^0 = 0.0002$), to the analytic solution and the numeric result of the deforming grid method. The KP model converges closely to the expected sharp-interface solution, whereas the CP model still exhibit a small measurable deviation at longer times. Figure 4c shows that the differences between KP and CP become small, for increasing values of the kinetic coefficient. Strong kinetic undercooling implies a slow moving interface, with a steep phase-field profile. The tendency of the CP model is therefore explained by the smaller values of the source term in the heat equation, at large values of $-T^0$.

The overall picture, anyway, indicates that both models yield acceptable values for $\Gamma(t)$, even at longer times, provided that $N \geq 250$ (interfacial thickness less than 0.005).

4.2. Temperature Profile

The temperature fields at time $t_0 = +0.08$ (shortly after the onset of the kinetic effect) is depicted in Figs. 5a,b,c. Figure 5a indicates that the results from the CP model exhibit large deviations from the classical sharp interface solution. As noted in Section 2.2.1, this could be improved by choosing a smaller value for the parameter a in Eq. (2.5), at the expense of increasing computational effort

TABLE I

Average Processor Times for the PF Simulations

N	Time step (seconds)	Mean CPU time per time step	Machine
100	5×10^{-3}	0.03 s	PC-AT 486/DX2 50 MHz
250	2×10^{-3}	0.3 s	SUN SPARC-2
500	5×10^{-4}	0.5 s	SUN SPARC-2
1000	1×10^{-4}	0.17 s	CRAY-2 XMP
2000	5×10^{-5}	0.23 s	CRAY-2 XMP

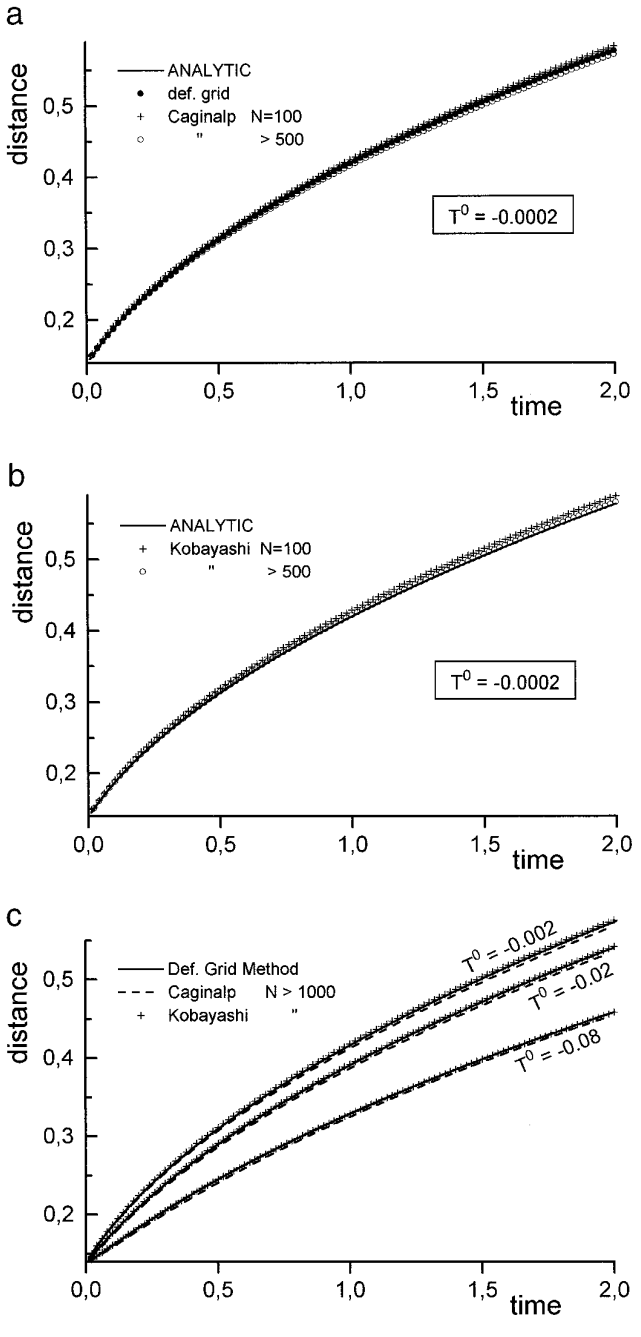

FIG. 4. Interface position as predicted by the CP (a) and KP (b) models. Also shown is the analytic Neumann solution and the numeric results of the deforming grid method. Both models yield almost the same results even for high values of the kinetic coefficient (c).

(finer meshes would be required for our fixed-grid discretization).

Figure 5b shows that the KP model yields essentially the same results as those obtained with the deforming grid method. Finally, in Fig. 5c we see that the differences between the two PF models become larger at higher values of the kinetic coefficient. It is interesting to note that the discrepancy of the CP solution at early times has little, if any, influence on the computed interface progression, as seen in the preceding section. These simulations were done at low values of the Stefan number $C(T_{\text{hot}} - T_{\text{cold}})/L$, so that the interface progression is mainly governed by the source term $\partial p/\partial t$ in the heat equation.

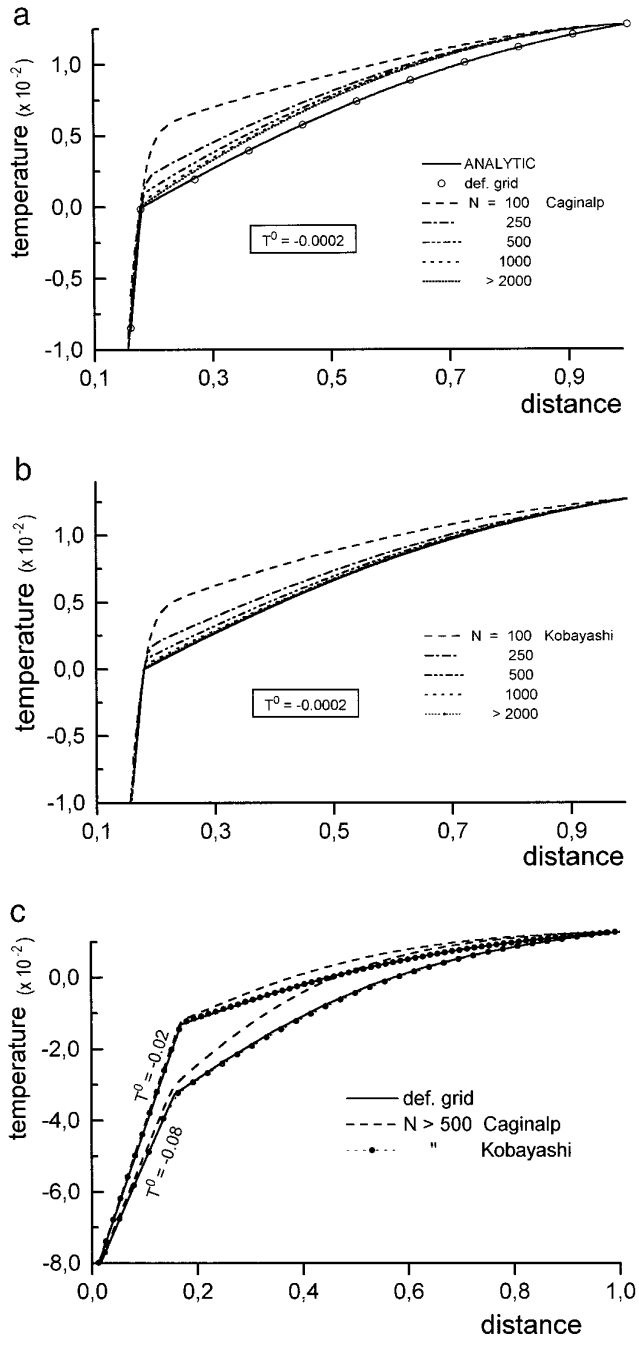

FIG. 5. PF results for the temperature profiles at time = 0.08, as obtained with the CP (a) and KP (b) models, for various values of the "numeric" interface thickness and of the kinetic coefficient (c).

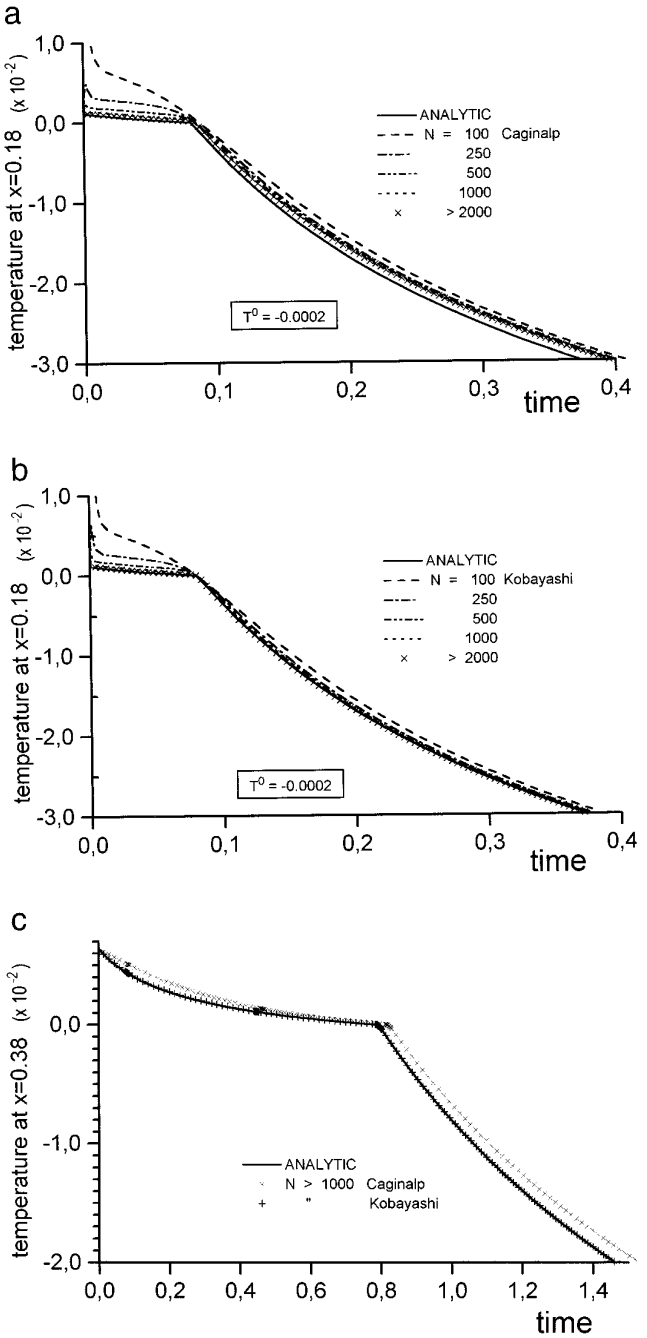

FIG. 6. The temperature history at $x = 0.18$ (a,b) and at $x = 0.38$ (c), for a very low value of the kinetic coefficient. The results of the PF models are compared with the analytic solution and with the numeric result of the deforming grid method.

4.3. Temperature History

The temperature history curves provide a severe check of the proper convergence of numerical methods for Stefan problems. The curves obtained from the PF equations, for $T^0 = 0.0002$, are shown in Figs. 6a,b, just ahead of the initial interface position, at $x = 0.18$, and in Fig. 6c at $x = 0.38$. It is clearly seen that the CP model exhibits a fairly larger deviation from the sharp-interface analytic solution, more than might be expected at such a low level of kinetic undercooling. Acceptable values for the temperature history require an interface thickness of less than 0.0025 ($N \geq 500$) in both the CP and KP models. Under that condition, the quantitative agreement between the results from the KP model and the analytical solution is rather impressive.

4.4. Phase versus Temperature Paths

At high levels of kinetic undercooling, even the simple unidirectional solidification considered here might exhibit bifurcation in the phase versus temperature paths. The results we have just seen for the temperature history suggest that the actual value of the undercooling, as obtained from the PF equations for a given value of the interface thickness ξ, is very sensitive to the model potential. We show in Fig. 7a a detail of the temperature history at the position $x = 0.30$, and in Fig. 7b, we show the corresponding phase versus temperature path, for an initial kinetic undercooling value of -0.08. It is seen that the liquid phase is supercooled well below the actual phase transition temperature. The temperature history predicted by the KP model agrees with the results of the deforming grid method, whereas in the CP model the liquid did not attain such low supercooling levels. During the simulation of alloy or solution solidification, the actual value of the attained liquid supercooling can have a dramatic impact on the dynamics of impurity trapping and compositional segregation.

4.5. Kinetic Undercooling at the Phase Front

The temperature at the interface ($p = 0$) versus time, for $T^0 = -0.002$, as obtained from the CP and KP models, is depicted in Figs. 8a,b, respectively, along with the expected value of the kinetic undercooling, $-(\alpha\sigma/\Delta s)(d\Gamma/dt)$. The interface velocity $d\Gamma/dt$ is obtained from the calculated interface position $\Gamma(t)$ by numeric differentiation. We also show the results from the deforming grid method. It is seen that both models yield satisfactory results, provided the interface thickness is less than 0.0025 ($N \geq 500$); for the same value of ξ, the numeric agreement of the KP model is clearly better than the one obtained with the CP model. A good qualitative agreement can be obtained for a "numeric interface" as coarse as 0.005 ($N = 250$).

At large values of the kinetic coefficient, the KP and CP models yield very distinct results, particularly at initial times (Figs. 9a,b). The results from the KP model agree well with the ones predicted by the deforming grid method, provided a small correction is made in the velocity exponent of the kinetic interface condition:

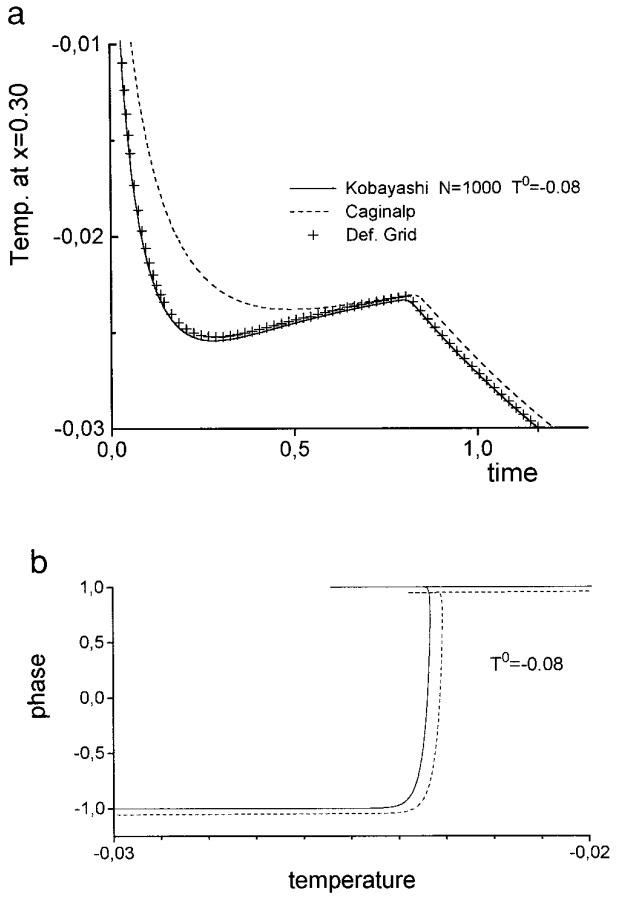

FIG. 7. A bifurcation in the phase versus temperature diagram, as obtained numerically with the PF models at $x = 0.30$. The temperature history (a) is represented in (b) as a path in the phase–temperature plane. The maximum undercooling predicted in the liquid phase is very sensitive to the model potential.

$$u = T_0 \left(\frac{v}{v_o} \right)^{\beta}. \tag{4.1}$$

Very small corrections in the value of β (0.98 for $T^0 = -0.02$ and 0.987 for $T^0 = -0.08$) bring the results from the KP model in agreement with the predictions of the deforming grid method. Such a small correction, of less than 2%, is probably irrelevant from the practical point of view. We therefore concluded that the KP model yields reliable results for the temperature at the phase front even at high levels of kinetic undercooling. It should be noted that no correction for β can account for the values predicted by the CP model.

5. CONCLUSIONS

The numerical results, obtained with a simple totally implicit fixed-grid control-volume discretization, favors the KP model for values of the kinetic coefficient commonly observed during actual solidification experiments. The KP model yields better values for the interface progression, temperature profiles, temperature histories, and phase-front temperatures, as compared to the CP model for the same interface thickness. Even at high values of the kinetic coefficient, the KP model remains close to the linear kinetic behavior, within the precision of our numeric calculations. Although correct qualitative behavior are obtained from both models for grids as coarse as 250 points, good numeric results seems to require a ''computational'' interface thickness of less than 0.0025 (within a typical macroscopic length scale of 1.0); for two- or three-dimensional calculations, that would require the use of adaptive methods, or else the use of vector-parallel machines. A length scale resolution of 10^{-3} to 10^{-4} is in fact required to handle complicated multidimensional solidification morphologies, if one hopes to resolve the geometry of dendrites—and those are precisely the kind of problems for which PF methods were

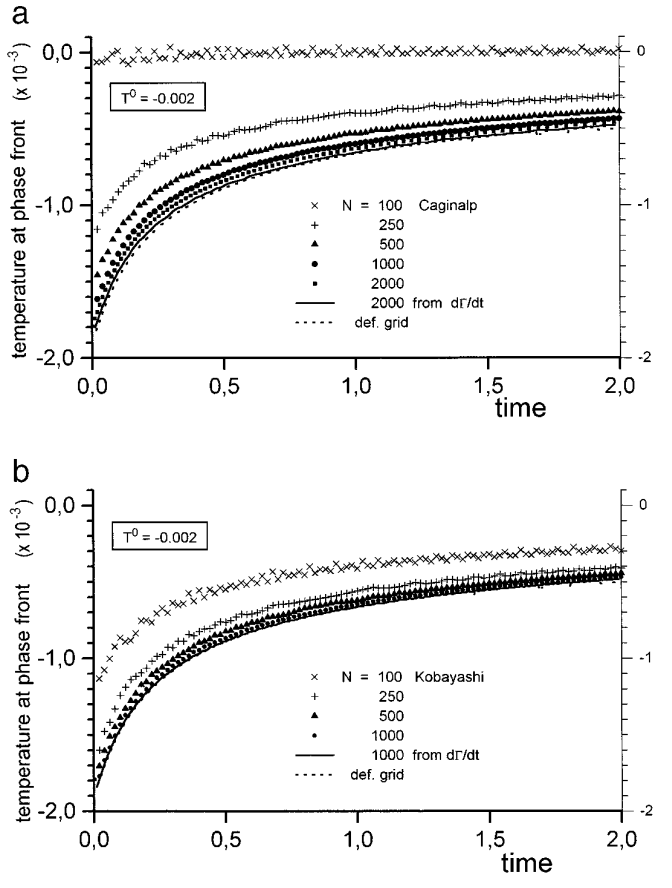

FIG. 8. Temperature at the interface ($p = 0$) during solidification, from the onset of the kinetic undercooling effect. The convergence of the PF results to the expected linear dependence on the interface velocity is shown in (a) and (b), for the CP and KP models, respectively, and agrees well with the prediction from the deforming grid method.

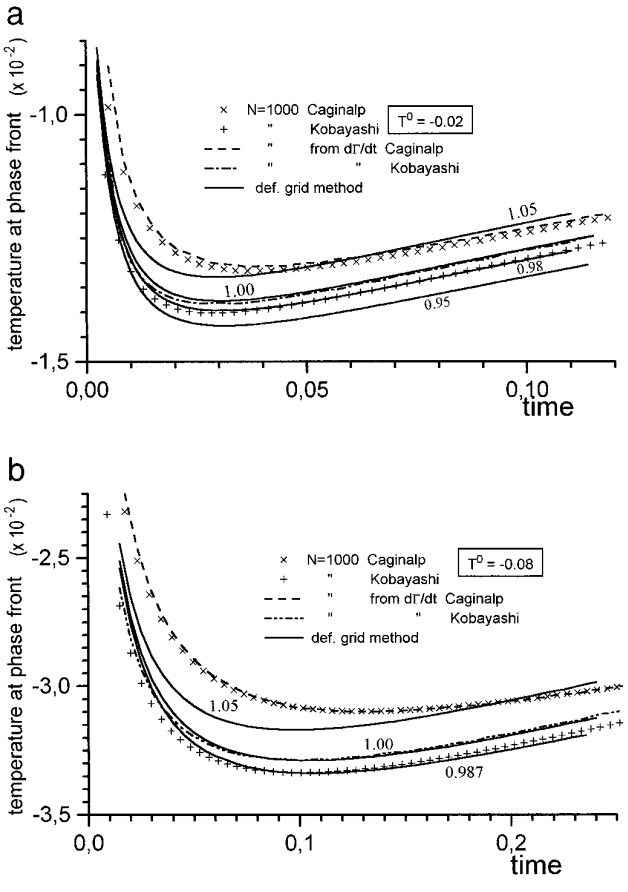

FIG. 9. Temperature at the phase front for high values of the kinetic coefficient, as compared to the values expected from the interface velocity. Small corrections in the velocity exponent (shown as numbers labeling the solid curves) were necessary to bring the results from the deforming grid method in almost complete agreement with the predictions of the KP model.

devised. In this sense, the PF runs with $N < 500$ might not be of much significance for real problems.

Note that no further effort was made here to relate the CP and KP parameters to the physical quantities occurring in actual solidification experiments. Our ''experimental'' benchmark was provided computationally, through reference to the results from a classical deforming grid method. When necessary, the PF parametrization can be related to the known sharp-interface material quantities, through an asymptotic analysis well described by Caginalp [17]. Further physical insight about the interfacial thickness required to model real sharp-interface problems can be obtained by a stability analysis performed by Braun *et al.* [26]. In many applications, good quantitative agreement is important, e.g., when dealing with problems of segregation during binary-alloy solidification, or impurity inclusion/trapping studies. In this respect, our numeric simulations provide further indication that the PF method allows for a reliable investigation of complex microscopic solidification phenomena with moderate computational effort.

ACKNOWLEDGMENTS

M. Fabbri would like to acknowledge a scholarshp from the Conselho Nacional de Desenvolvimento Cientifico e Tecnologico, CNPq, Brazil. This work was also supported by a resources grant from the Minnesota Supercomputer Institute, Minneapolis, MN, USA, and by the Fundação de Amparo à Pesquisa do Estado de São Paulo (FAPESP), Brazil.

REFERENCES

1. G. Caginalp, *Arch. Rat. Mech. Anal.* **92,** 205 (1986).
2. G. Caginalp and J. Lin, *IMA J. Appl. Math.* **39,** 51 (1987).
3. G. Caginalp and E. A. Socolovski, *J. Comput. Phys.* **95,** 85 (1991).
4. J. S. Langer, in *Directions in Condensed Matter Physics* (World Scientific, Singapore, 1986), p. 164.
5. J. B. Collins and H. Levine, *Phys. Rev. B* **31,** 6119 (1985).
6. R. Kobayashi, *Physica D* **63,** 410 (1993).
7. A. A. Wheeler, W. J. Boettinger, and G. B. McFadden, *Phys. Rev. A* **45**(10), 7424 (1992).
8. A. A. Wheeler, W. J. Boettinger, and G. B. McFadden, *Phys. Rev. B* **47**(3), 1893 (1993).
9. G. Caginalp and W. Xie, *Phys. Rev. E* **48**(3), 1897 (1993).
10. G. Caginalp and J. Jones, *Ann. Phys.* **237,** 66 (1995).
11. O. Penrose and P. C. Fife, *Physica D* **43,** 44 (1990); **69,** 107 (1993); see also the discussion between G. Caginalp, O. Penrose, and P. C. Fife in *Appl. Math. Lett.* **5**(2), 93 (1992); **5**(6), 99 (1992).
12. G. Caginalp and J. Jones, in *On The Evolution of Phase Boundaries* (Springer-Verlag, New York, 1992), p. 29.
13. P. C. Hohenberg and B. I. Halperin, *Rev. Mod. Phys.* **49,** 435 (1977).
14. B. T. Murray, W. J. Boettinger, and G. B. McFadden, *Computation of Dendritic Solidification Using a Phase-Field Model,* preprint of the ''29th ASME/AIChE National Heart Transfer Conference, Atlanta, GA, Aug. 1993.''
15. H. Lowen, J. Bechhoefer, and L. S. Tuckerman, *Phys. Rev. A* **45,** 2399 (1992).
16. S. M. Allen and J. W. Cahn, *Acta Metall.* **27,** 1085 (1979).
17. G. Caginalp, *Phys. Rev. A* **39**(11), 5887 (1989).
18. R. Kobayashi, *Exp. Math.* **3,** 59 (1994).
19. A. A. Wheeler, B. T. Murray, and R. J. Schaefer, *Physica D* **66,** 243 (1993).
20. S.-L. Wang *et al., Physica D* **69,** 189 (1993).
21. G. Caginalp and X. Chen, in *On the Evolution of Phase Boundaries* (Springer-Verlag, New York, 1992), p. 1.
22. H. S. Carslaw and J. S. Jaeger, *Conduction of Heat in Solids,* 2nd ed. (Clarendon Press, Oxford, 1959), p. 285.
23. S. V. Patankar, *Numerical Heat Transfer and Fluid Flow* (McGraw–Hill, New York, 1980).
24. J. T. Lin, *SIAM J. Numer. Anal.* **25,** 1015 (1988).
25. V. R. Voller and S. Peng, A unification of fixed and deforming grid schemes for solution of the Stefan problem, *Comput. Mech.,* submitted.
26. R. J. Braun *et al., Phys Rev. E* **49,** 4336 (1994).